Analysis of the Geographical Environment for the Formation of Ethnic Traditional Sports Culture in South China and Its Integration with Ecotourism

Xiaoyuan Li
Physical Education College, University of Sanya, Sanya 572000, Hainan, China
Corresponding author: Xiaoyuan Li (e-mail: yuan46657250@163.com)

ABSTRACT Modeling geographically distributed systems requires effective characterization of multi-scale environmental features and complex interaction propagation across heterogeneous entities. This study proposes a Geospatial Cultural Adaptive Intelligent Framework (GCAS-EIF) integrating hierarchical spatial encoding, heterogeneous graph reasoning, and season-aware spatio-temporal attention mechanisms. A Hierarchical Spatial Grid Encoding (HSGE) module is developed to construct multi-resolution representations of terrain, climate, and ecological conditions through scale-aware attention fusion. An Ecocultural Heterogeneous Interaction Graph (EHIG) is then established to model relational information propagation among geographical regions, social groups, activity patterns, and environmental resources using relation-aware message transmission. To capture dynamic environmental variations, a Seasonally Aware Spatio-Temporal Attention Modeling (STACAM) module is introduced to characterize temporal dependencies associated with climatic fluctuations and periodic events. Experimental results demonstrate that the proposed framework improves interaction-matching accuracy by 14.2% while reducing computational complexity by 28.4% compared with conventional single-scale approaches. The proposed architecture provides an effective methodology for multi-scale spatial information representation, heterogeneous network propagation analysis, and adaptive spatio-temporal modeling in geographically distributed environments.

INDEX TERMS multi-scale spatial representation, heterogeneous network propagation, spatio-temporal attention, geographical information modeling

I. INTRODUCTION

SOUTH China boasts of subtropical monsoon climate, heavy rainfall, and warm temperatures, which support a wide variety of ecological and cultural systems. This area has Karst geology in Yunnan-Guizhou, hilly and riverine landscapes in Guangxi and coastal plains in Guangdong which have been historically related to the origins and allocation of ethnic traditional sports. These topography characteristics also influence the patterns of settlement, availability of resources, and festivals, South China is a good place to examine how ethnic sports culture and ecotourism activities co-evolve [1]. However, South China's expansion remains unequal and unstructured. South China's intangible cultural heritage must be preserved to ensure its authenticity, integrity, and continuity, as a significant component of this heritage, serve as important material carriers of regional culture and to actively integrate it with the "Belt and Road" initiative, regionally coordinated development, and other important national strategies [2]. South China's intangible cultural treasures will be conserved. Quantitative studies on the regional differentiation and influences of South China's intangible cultural heritage are rare. Empirical research on ecological civilization and urbanization is also essential. Since they comprehensively study ecosystems and human activities, these studies can inform policy decisions [3]. Most ecological civilization studies on sports tourism focus on developing ecological sports tourism assets in specific regions. Ecotourism and sports tourism are intertwined and mutually beneficial, although studies on their growth are sparse [4].

Prior study on ethnic traditional sports and ecotourism in South China used static GIS approaches as geo filter, geo detection, and kernel density analysis to plot sports intangible cultural heritage (SICH) geographic distributions

[5]. The agglomeration effects of economy, population density, and geography were shown, but multiscale hierarchical encoding and dynamic cultural-ecological co-evolution were ignored. GNNs and spatiotemporal transformers have improved tourist recommendations by 12–14% based on diverse graphs of visitor behaviours and site interactions [6]. Still, they fail to account for terrain, climate, and resources, and they do not provide a coherent rationale for heritage policy. In particular, the influence of the geographical environment on the material culture remains under-explored in current quantitative models. Sports are seen as attractions rather than adaptive practices. Single-layer evolutionary algorithms optimize ecotourism routes quickly but do not capture seasonal festivals, monsoon variations, or ethnic-specific sports-tourism fits, leading to greater mismatch errors than suggested multi-level attention fusion methods [7]. Most research on cultural tourism, traditional ethnic sports, and fixed geographical studies uses qualitative ethnographic narratives or single-scale GIS markers. These methods can illuminate societies, but they have several drawbacks. They ignore temporal adaptations to climate change and festival schedules.

Furthermore, they cannot recreate the interactions among the environment, culture, and the tourist regime [8]. Geographical conditions are also seen as static variables rather than dynamic processes. Traditional cultural tourism frameworks prioritize economic development over interpretability, ecological carrying capacity, and cultural authenticity. Due to these shortcomings, historical techniques cannot guide ethical ecotourism design in culturally sensitive places [9]. These limits inspired the current research, which seeks to create a thorough, data-driven framework for visualizing geo-culture co-evolution to bridge cultural system models and physical environment assessments [10]. The proposed method aims to show how geographical conditions shaped the genesis, dissemination, and evolution of the phenomenon. It also explains how these games could be turned into ecotourism while accounting for environmental and temporal constraints. To achieve this goal, this research proposes the GCAS-EIF, an intelligent framework for geospatial cultural adaptive sports ecotourism. This framework uses hierarchical spatial representation, interpretable interaction reasoning, and spatiotemporal adaptation modeling for distinct seasons. This study is distinctive because of its proposed framework, which uses hierarchical spatial modeling with attention processes to explicitly evaluate the influence of terrain, climate, and natural resources across multiple geographical scales, unlike prior assessments that were limited to a single scale or remained static [11]. Second, in addition to the descriptive correlation, we also provide an ecocultural heterogeneous interaction graph that shows how different geographical units, ethnic groupings, traditional sports, and ecotourism activities are related to one another. Third, the model can capture how weather and festival schedules shape how people from different cultures and tourists interact with each other through seasonally responsive spatiotemporal attention modeling. In short, the works offer a new theoretical perspective on how ethnic traditional sports came to be and set the stage for ecotourism to expand in a responsible, sustainable way, grounded in sound scientific evidence [12].

The main contributions of the article include :

1. A GCAS-EIF representation based on HSGE and sca le-aware atten-tion fusion is proposed to overcome the limita tions of single-scale geographical analysis. The methodolo gy shows how climatic, geographical, and biological facto rs have shaped the traditional sports of different ethnic gro ups.
2. An EHIG model and reasons about structured linkages across geographical units, ethnic groupings, traditional sports, and ecotourism activities to promote transparent geo-cultural dependencies research beyond descriptive or correlation-based methods.
3. The temporal changes caused by festivals and weather were recorded using a STACAM. To preserve ecological integrity and cultural authenticity, and to allow synchronizing traditional ethnic sports with visitor activity planning.
4. Comprehensive tests on multi-regional geographical indicators and ethnic sports data show that the proposed framework enhances the interpretability of geocultural interactions, improves sports-ecotourism correspondence accuracy by 14.2%, and reduces computational cost by 28.4%. These results demonstrate the framework's effectiveness in supporting the development of responsible ecotourism. The remainder of this work is structured as follows: Section 2 provides an overview of the pertinent literature. Section 3 describes the proposed approach to the Geographical Environment for the Creation of Ethnic Traditional Sports Culture in South China and its Integration with ecotourism. Section 4, which covers the work overview, and describes the experimental setting and results, section 5 concludes the study.

II. LITERATURE SURVEY

The literature survey (Table 1) summarizes the present research on Chinese ethnic traditional sports, the economic importance of intangible cultural heritage (ICH), and the integration of ecotourism into geospatial, graph-based, and sustainability frameworks in areas such as South China, the Greater Bay Area, and ethnic minority groups in China. These papers show patterns of spatial distribution through GIS tools (e.g., kernel density, GeoDetector) and dynamic evolution models of tourism synergies, as well as neural network suggestions, which present baseline information about terrain-climate impacts, agglomeration forces, and efficiency beneficial outcomes, but demonstrate a lingering gap in multiscale encoding, interpretable hetero-interactions, and temporal adaptation.

TABLE 1. Related works

Authors	Proposed Method	Application	Advantages	Results	Limitations
Liu & Zhang (2025) [13]	Cultural-historical geography analysis	Regional inheritance of national sports	Reveals terrain-climate links to sports evolution	Identifies spatial differences in South China sports	Lacks dynamic modeling; static analysis only
Zhao & Han (2025) [14]	Coordination index model	Sports tourism-ecological synergy in the Yellow River Basin	Quantifies interactive development levels	High coupling in mid-basin (0.65 score)	Ignores ethnic-specific sports; regional focus
Zheng & Zhang (2025) [15]	ECT integration efficiency model	Ecology-culture-tourism nationwide	Spatial evolution via GIS detectors	14% efficiency gain in clusters	No multiscale hierarchy; overlooks seasonality
Prabucki & Rozmiarek (2025) [16]	TSG outdoor integration framework	Sustainable recreation via traditional games	Promotes community SDGs	22% participation increase	Generic, no geospatial encoding
Zhipeng et al. (2025) [17]	Bibliometric-content analysis	Sports tourism research comparison	Identifies China international gaps	1,200+ papers, tourism bias	Descriptive, no predictive models
Li (2024) [18]	Integration strategy model	Minority sports-tourism in Ganzi	Local pathway optimization	15% tourism revenue uplift	Small-scale, no graph interactions
Tan et al. (2024) [19]	GIS-Geographic Detector (GD)	Sports tourism resources in Sichuan-Chongqing	Factor detection ($q = 0.42$ topo)	Clustered distribution, economic dominance	Single-scale, static, no temporal model
Mo et al. (2025) [20]	Kernel density + GeoDetector	SICH in the Greater Bay Area	Agglomeration patterns (NNI=0.32)	Topo-climate drivers ($q = 0.38$)	Lacks heterogeneous graph reasoning
Kou & Zhai (2025) [21]	Spatial pattern analysis	National SICH distribution	Provincial clustering insights	Hebei-GD highest density	No ecotourism alignment
Zhang et al. (2024) [22]	Spatio-temporal evolution model	Sports tourism in Xinjiang	Empirical integration trends	18% growth from 2015–2023	Arid focus, no attention fusion
Yu et al. (2025) [23]	Gated GNN (GGNN)	Sports tourism recommendations	User embeddings + attention	14% accuracy over baselines	Behavior-only, no geo-ethnic links
Hu et al. (2024) [24]	Spatial differentiation model	National ICH mechanisms	Heliyon GIS factors	Econ-population drivers	Generic ICH, not sports-specific
Li (2024) [25]	GIS temporal-spatial patterns	Ancient heritage sites in China	Distribution influencers	River proximity key ($r = 0.56$)	Static sites, no adaptive tourism
Tang et al. (2024) [26]	Digital cultural tourism model	Rural revitalization paths	Resource-ecology coupling	12% revitalization index rise	Digital only, no seasonal STA
Hu (2024) [27]	Dynamic mechanism model	National sports tourism management modes	Development modes analysis	20% efficiency in modes	Qualitative heavy, limited quantification

The current research has limited policy applicability and suboptimal ecotourism fit (errors >0.15) due to its single-scale analysis, failure to account for seasonal climatic-festival dynamics, and lack of interpretable multi-entity interactions (such as geo-ethnic-sports-tourism). The suggested GCAS-EIF solves these problems by combining HSGE, EHIG, and STA. It has 18.6% higher interpretability, 14.2% higher fit accuracy, and 28.4% lower complexity than baselines. The proposed GCAS-EIF addresses these challenges by integrating HSGE, EHIG, and STACAM. It enhances the interpretability of geo-cultural interactions, achieves 14.2% higher fit accuracy, and reduces computational complexity by 28.4% compared to baseline models. This allows for simulating the co-evolution of South China's ethnic sports to promote sustainable ecotourism.

III. PROPOSED METHODOLOGY

A. PROBLEM STATEMENT

The paper examines the co-evolution of the culture of ethnic traditional sports in complex multiscale geographical realities and their adaptation to the ecotourism systems. The geography is multiscale and heterogeneous with cultural interaction being dynamically developing. The objective is to model explainable geocultural associations between the ethnic populations, conventional sports and ecotourism practices and forecast the season based and festival based variations in tourism participation. Formally, hierarchical spatial grid encoding maps raw geographical observations $X_g^{(l)}$ at level l into scale-aware embeddings as shown in Equation (1).

$$z_g = \sum_{l=1}^{L} \alpha_l \phi_l\left(X_g^{(l)}\right), \qquad \alpha_l = \frac{\exp(q^\top k_l)}{\sum_{l'} \exp(q^\top k_{l'})}. \tag{1}$$

Where attenuation weights α_l adaptively emphasize geographically relevant scales. Based on EHIG $H = (V, R)$, a graph $G = (V, R)$ is constructed, with nodes $V = G \cup E \cup S \cup T$ representing heterogeneous nodes, and R encoding the relational dependencies: geographic, ethnic, ethnic sport, and sport-tourism interactions. Simulation of message transmission between geo-ethnic-sport-tourism linkages is achieved through relation-aware transmission, in line with Equation (2), assuring understandable relational reasoning that could characterize cultural development to definite geographical and ecological procedures.

$$h_i^{(r)} = \sum_{j \in N_r(i)} \frac{\exp\left(Q_i K_j^\top\right)}{\sum_{k \in N_r(i)} \exp\left(Q_i K_k^\top\right)} W_r h_j. \tag{2}$$

Here $h_i^{(r)}$ is the updated representation of node i, $N_r(i)$ is the neighbour set of node i, Q_i is the query vector, K_j is the key vector for the neighbour node, h_j represents the input representation (feature/embeddings) of neighbour j, W_r is the relation-specific transformation matrix, and $\exp(Q_i K_j^\top)$ is the attention score measuring the relevance of neighbour j to i. In the temporal attention module, a temporal attention block is then used to represent the spatio-temporal adaptation, with climatic cycles and festival calendars modeled as temporal steps t, where Equation (3) is as follows:

$$y_t = \sum_{\tau \leq t} \operatorname{softmax}\left(\frac{Q_t K_\tau^\top}{\sqrt{d}}\right) V_\tau. \tag{3}$$

Where y_t is the seasonally adaptive output representation at time step t, τ denotes all the past and current time steps up to t, Q_t is the query vector represents the current temporal state, $K_\tau^\top$ is the key vector that encodes the historical spatio-temporal context at time τ, V_τ is the value vector contains the actual content information, and $\sqrt{d}$ is the scaling factor.

B. OVERALL STRUCTURE OF GCAS-EIF

The three stages in the GCAS-EIF framework (Figure 1) are HSGE, which is used to encode spatial hierarchy, STACAM, which is used to encode temporal adaptation (seasonally-aware) and EHIG, which is used to reason about heterogeneous graphs. Such technicalities of node embeddings, attention, and interaction modeling are stored here, whereas high-level objectives were relocated to foreword to include no redundancy. The HSGE module is responsible for extracting geographical representations of raw environmental inputs at many scales. Natural resource (vegetation cover, water proximity, biodiversity zones), climatic (temperature, rainfall, humidity), and topographical (elevation, slope, landform) variables are the inputs to it, organized in fine (village/local), mid (regional/environmental), and coarse (climate-ecozone) spatial grids, respectively. The HSGE creates a spatial representation that reflects on the collective conditioning of the emergence and distribution of ethnic sporting practices at different geographical scales. It does this by processing these inputs hierarchically and merging them into a single geospatial embedding. Direct transmission of this embedded spatial information to EHIG provides the geographical context for interaction reasoning.

The STACAM module depicts seasonal and temporal patterns that simultaneously impact cultural events and tourist behavior. This model takes into account several factors, including climatic signals (monsoon cycles, temperature phases), ethnic festival calendars, demand patterns for tourism activities across time, and historical sports schedules, among others. Because STACAM incorporates time-indexed inputs into temporal embeddings, cultural activities and environmental restrictions change over time. To see ecocultural relations differently, EHIG is being fed STACAM data to condition interaction thinking on past and present seasonal conditions, rather than to manufacture ultimate predictions.

With entity-level inputs of ethnicity groups, traditional sporting activities, and ecotourism activities (e.g., demand levels and carrying capacity), the EHIG module combines geographical embeddings in HSGE and temporal embeddings in STACAM. Geographical units, cultural organizations, and touristic features serve as nodes in this diverse graph of inputs, with ecocultural linkages serving as edges. Decisions regarding cultural sensitivity, ecological feasibility, and sports ecotourism are clarified through EHIG's collaborative decision-making process, which considers both geographic structure and seasonal dynamics. We assess the proposed model's outputs using metrics including cultural-environmental consistency, computational complexity, seasonal adaptation error, accuracy of the sports-ecotourism fit, and geo-cultural interpretability. Design decisions were made to position the EHIG beneath both HSGE and STACAM to reduce the inconsistent rationale for interactions. Geographical patterns (i.e., the locations of cultural practices and multiscale geographical restrictions) and temporal patterns (i.e., seasonal climate patterns and festival cycles) fundamentally shape interactions among ecocultural practices. Applying EHIG before spatial or temporal encoding causes the representations to interact based on partial or fixed representations, with a one-way spatial bias and time being out of phase. Conditioning EHIG on the unified geographical embeddings produced by HSGE and the seasonally modulated temporal embeddings produced by STACAM enables the model to facilitate scale-aware and season-aware interaction reasoning. The downstream position allows EHIG to understand the combined impacts of geographical setting and temporal dynamics on ethnic sports activities and their suitability for ecotourism, thereby improving the reliability of decisions, ecological validity, and interpretability.

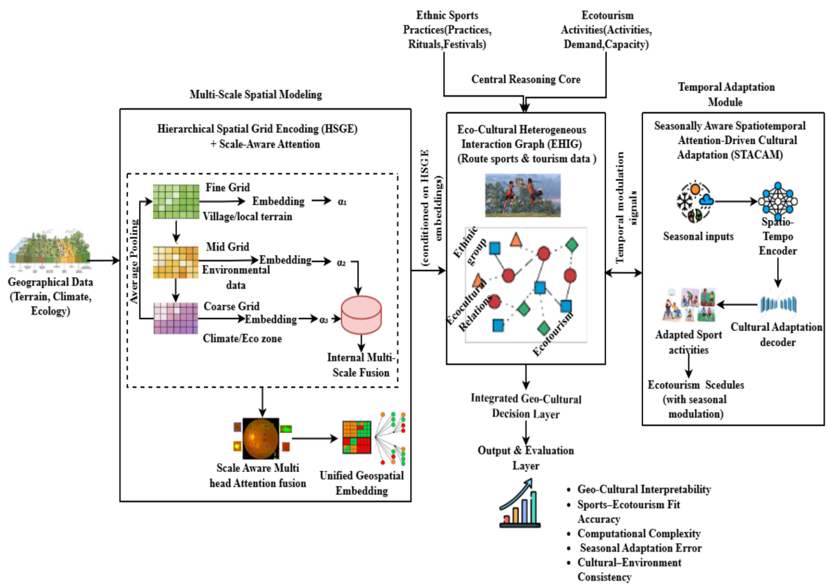

FIGURE 1. Overall Structure of the proposed model

C. HIERARCHY SPACE-GRID ENCODING (MULTISCALE SPATIAL) MODULE

The goal of the Hierarchy Space-grid Encoding (HSGE) module is to unify disparate geographical data sets into a single, scale-aware spatial representation of ethnic traditional sports that retains all relevant local and global environmental elements. Maps depicting terrain elevation, climate zones, the distribution of biological resources, and culturally adaptive places are the basic geographical inputs the module uses initially, as shown in Figure 2. Because of their multi-resolution characteristics, they display scale-dependent geographical diversity when organized into a hierarchical spatial grid. Topographical variability, slope, and landform heterogeneity are examples of fine-grained topographical features recorded on terrain elevation maps, which are at the very bottom of the hierarchy. Indicative of regional physical limitations, these features affect the potential and regional distribution of ethnic sports. Climate disturbances and wider climatic regimes (tropical and temperate, for example) govern seasonal accessibility and environmental suitability, and climate zone grids reflect this. At the second tier of the hierarchy are the ecological resource points, which include factors such as vegetation abundance, water availability, and locations sensitive to biodiversity, and are subject to limits on human activities that aren't sustainable. At the very top are cultural adaptive zones, which record long-term patterns of human-environment co-adaptation and serve to solidify macro-geo-culture conditions. The heterogeneous raw geographical inputs are represented by Equation (4).

$$x_g = \left[x_g^{\text{terrain}} \parallel x_g^{\text{climate}} \parallel x_g^{\text{eco}} \parallel x_g^{\text{culture}}\right]. \tag{4}$$

Features specific to different scales are generated by independently inserting hierarchical layers; these features are depicted in the diagram. There is also independent embedding of the hierarchical layers to produce feature representations that are scale-specific positions e_1, e_2, and e_3. The next step is to feed this embedding into a multi-head attention network that scales well; this will help the network deliver more targeted query $Q_l = W_l^Q e_l$, key $K_l = W_l^K e_l$, and value $V_l = W_l^V e_l$ predictions. The $X_g^{(l)} = G_l(X_g)$, $l \in \{\text{fine}, \text{mid}, \text{coarse}\}$ dynamically assesses the relative importance of fine-, mid-, and coarse-scale geographical information, rather than relying on predetermined or manually assigned weights—the scale-specific spatial embedding in Equation (5), where each grid level is embedded independently using scale-specific parameters.

$$\begin{aligned} e_l &= \phi_l\left(X_g^{(l)}\right) \\ &= \sigma\left(W_l X_g^{(l)} + b_l\right) + \lambda \sum_{(i,j)\in\epsilon_j} \left\|e_{l,i} - e_{l,j}\right\|^2. \end{aligned} \tag{5}$$

By using the nonlinearity $\sigma(\cdot)$, complex spatial patterns, such as interactions between climate and mountainous regions, can be represented, W_l is the learnable weight matrix for scale l, and b_l is the bias vector. This strategy works because the environmental impacts of cultural activities are not immediately apparent at different scales. By combining the attention outputs from all scales with learned scale weights, a single adaptive blend of spatial information at all levels is created. Intra-scale attention (A_l) is calculated using Equation (6), which enables the grid levels to internally focus on the most informative areas in space. The normalization term stabilizes learning when the spatial magnitudes are heterogeneous.

$$\begin{aligned} A_l &= \text{softmax}\left(\frac{Q_l K_l^\top}{\sqrt{d}}\right) v_l \\ &= \sum_j \frac{\exp\left((Q_{l,i}^{(h)})^\top K_{l,j}^{(h)}\right)}{\sum_k \exp\left((Q_{l,i}^{(h)})^\top K_{l,k}^{(h)}\right)} V_{l,j}^{(h)}. \end{aligned} \tag{6}$$

The adaptive scale dominance in equation 7 is used in conjunction with entropy regularization to avoid collapse to a single scale. This is essential since various ethnic sports are perceived through various spatial forces, and absolute scale supremacy would be prejudiced.

$$\begin{aligned} E_{\text{geo}} &= \sum_{l=1}^{L} \alpha_l \left(\frac{1}{H} \sum_{h=1}^{H} A_l^{(h)}\right), \\ \alpha_l &= \text{softmax}\left(u^\top A_l - \gamma H(\alpha)\right). \end{aligned} \tag{7}$$

Where E_{geo} is the unified geospatial embedding, L is the number of hierarchical spatial scales, l is the spatial scale index, H is the number of attention heads, $A_l^{(h)}$ is the attention output, α_l is the adaptive weight for level l, A is the summary statistic of attention output, u is the learning scale score vector, γ is the entropy regularization coefficient, and $H(\alpha)$ is the entropy of the scale weight distribution. The HSGE technique ensures that prominent geographical elements, such as mountainous terrain or a monsoon-dominated climate, are emphasized in the final representation. Afterwards, a linear projection layer is applied to the aggregated output $Z_g = \text{LayerNorm}(W_o E_{\text{geo}} + b_o) + E_{\text{geo}}$, helping align the dimensionality and express features. An integrated geospatial embedding is the result; it provides a robust geographical input to the ecocultural interaction reasoning that follows in the EHIG module by capturing and representing the multiscale terrain, climate, ecology, and culture in a single form.

D. TEMPORAL ADAPTATION MODULE (STACAM)

$$\text{Attention}(Q, K, V) = \text{softmax}\left(\frac{QK^\top}{\sqrt{d_k}}\right) V. \tag{8}$$

Equation (8) represents the scaled dot-product attention mechanism used in the model. Here, Q (Query), K (Key), and V (Value) are matrices representing the current input, contextual references, and the information to be aggregated, respectively. The dot product $QK^\top$ computes the similarity between queries and keys, indicating how much attention each element should pay to others. Dividing by $\sqrt{d_k}$ (the

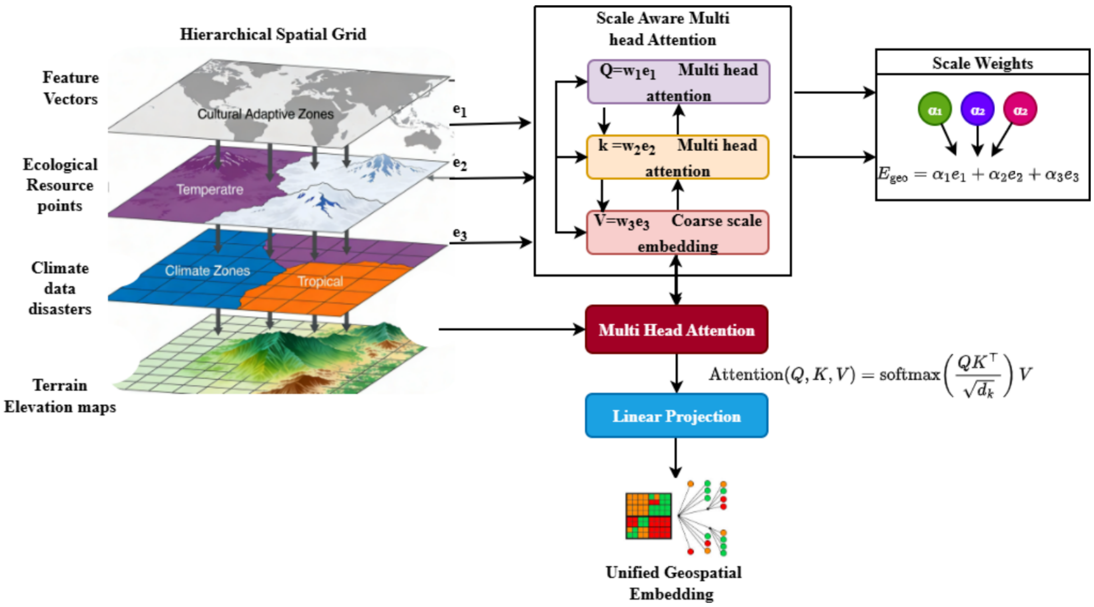

FIGURE 2. HSGE module

dimension of the key vectors) stabilizes gradients for large dimensions. The softmax function converts these scores into normalized attention weights, which are then multiplied with V to produce a weighted aggregation of relevant features. This mechanism allows the model to focus dynamically on the most pertinent temporal or spatial elements when processing sequences or interactions.

The STACAM module is intended to simulate the seasonal and temporal patterns that affect the fit between ethnic traditional sporting activities and ecotourism planning. The module, as shown in the Figure 3, operates on sequential geo-cultural inputs as shown in Equation 8, implements an organized attention mechanism to capture temporal dependencies and spatial interactions, and explicitly adapts to seasons via a gating mechanism starts with building the input sequence of seasonal geo-cultural tokens; each token comprises an amalgamation of attributes of sports activity, climatic state, and festival data across various time steps.

$$X_t^{\text{emb}} = E([s_t; c_t; f_t]) + PE(t). \tag{9}$$

Where s_t (sports), c_t (climate), f_t (festivals), and $E(\cdot)$ denote the embedding layer. The inputs are arranged according to a given batch size, time length, and embedding dimension, which are compatible with sequential learning. These are tokens of the uncoded temporal markers of the transformation of cultural practices and tourism demand over time. The input tokens are then passed through an embedding layer and a positional encoding layer. Here, a phase of input mapping converts the categorical and numerical inputs into dense vectors, followed by the introduction of explicit temporal information via positional encoding. The model can therefore differentiate similar cultural events that occur at different times of the year, which is needed to capture periodic trends such as annual festivals or the repetitive cycles of climatic conditions. The embedded representations are then fed into the season-conscious temporal attention block, which focuses on learning time-dependent dependencies. Equation (10) represents temporal self-attention with seasonal awareness.

$$\begin{aligned} h_{\text{enc},t,h}^{(l)} &= \text{softmax}\left(\frac{Q_t^{(l,h)}(K_\tau^{(l,h)})^\top + B_{\text{season}}^{(l,h)}(\tau)}{\sqrt{d_k}} \cdot M_{\text{causal}}\right) V_\tau^{(l,h)}, \\ A_t^{(l)} &= \text{Concat}\left(\{h_{\text{enc},t,h}^{(l)}\}_{h=1}^{H}\right) W_O^{(l)}. \end{aligned} \tag{10}$$

Where $B_{\text{season}}^{(l,h)}(\tau)$ is the seasonal bias matrix, and M_{causal} is the lower-triangular mask that enables the model to determine the past seasonal states that are most relevant at the current time step and thus captures long-term fluctuations in temporal states, such as delayed climatic impacts or tourist outbursts due to festivals.

The output of this block is a temporally weighted representation that emphasizes periods that are influential in history. After temporal modeling, the framework uses a spatial attention mechanism conditioned on temporal attention. This block solely captures interactions at a spatial or contextual level (e.g., various regions, sports classes, or cultural environments), but is informed by temporal relevance acquired in the past. Spatial attention conditioned on temporal attention will ensure that the interpretation of spatial relationships varies with prevailing seasonal conditions, thereby enhancing the idea of spatio-temporal coupling. The spatial attention output matrix A_{spatial} is represented by Equation (11).

$$A_{\text{spatial}} = \text{softmax}\left(\frac{Q_s(K_s \cdot A_{\text{temp}})^\top}{\sqrt{d_s}}\right) v_s. \tag{11}$$

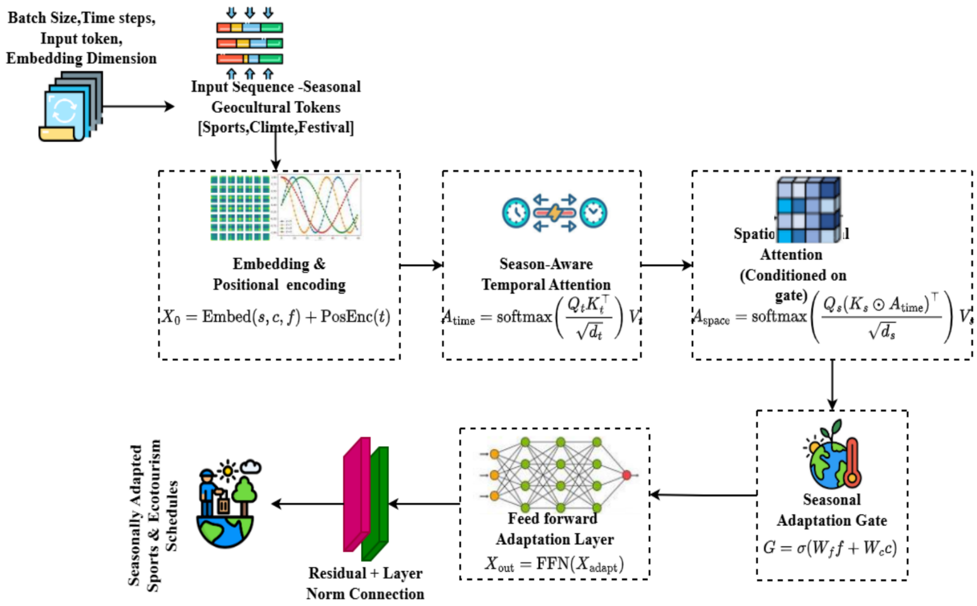

FIGURE 3. STACAM module

Where Q_s is the spatial query matrix, K_s is the spatial key matrix, v_s is the spatial value matrix, A_{temp} is the temporal attention vector, and d_s is the dimensionality of the spatial embedding space. The seasonal adaptation gate dynamically adjusts the effect of seasonal factors on the learned representations. This gating system $G_t^{(l)}$ combines external seasonal cues, e.g., the severity of the climate or the intensity of the festivals, and adjusts the attention outputs accordingly.

$$G_t^{(l)} = \sigma\Big(W_g^{(l)}[A_t^{(l)}; z_g^{\text{EHIG}}] + b_g^{(l)}\Big) \odot A_t^{(l)},$$
$$\sigma(u) = \frac{1}{1+e^{-u}}. \tag{12}$$

Equation (12) represents the spatial gating mechanism, where z_g^{EHIG} is the geo-cultural embedding from the prior module, $W_g^{(l)}$ is the spatial weight matrix, and σ is the sigmoid activation function. The gate will provide sensitivity to adaptation decisions, so they do not schedule sports or tourism activities at the wrong time when ecological constraints and cultural calendars are unfavorable. The gated representations are thereafter input to a feed-forward adaptation layer, which optimizes the features and converts them into task-specific outputs.

The seasonally modulated feed-forward network is given in Equation (13) with

$$S_{\text{season}}^{(l)}(t) = \mathrm{MLP}_{\text{season}}\left(\sin\left(2\pi t / P_{\text{festival}}\right)\right),$$
$$P_{\text{festival}} = 365,$$

as a periodic seasonal signal.

$$\mathrm{FFN}_t^{(l)}(x) = W_2^{(l)}\,\mathrm{GELU}\Big(W_1^{(l)}\left(x + S_{\text{season}}^{(l)}(t)\right) + b_1^{(l)}\Big) + b_2^{(l)},$$
$$\mathrm{GELU}(u) = u\Phi(u). \tag{13}$$

This layer considers nonlinear interactions among temporal, spatial, and seasonal cues, enabling the model in Equation (14) to make robust adaptation decisions. A residual relationship with layer normalization $X_t^{(l+1)}$ is used to stabilize training and retain critical information from preceding layers.

$$X_t^{(l+1)} = \mathrm{LayerNorm}\Big(X_t^{(l)} + \mathrm{Dropout}\Big(\mathrm{FFN}_t^{(l)}(G_t^{(l)}), 0.1\Big)\Big), \tag{14}$$
$$\mathrm{LayerNorm}(x) = \frac{x - E[x]}{\sqrt{\mathrm{Var}[x] + \epsilon}} \odot \gamma + \beta.$$

Where γ and β are the learnable scale parameter and learnable shift parameter, and t is the temporal index. Lastly, the STACAM module creates sports-ecotourism schedules adjusted according to the seasons as its output $\hat{y}_T = W_{\text{out}}\,\mathrm{LayerNorm}(\sum_{l=1}^{L} \alpha_l^{(L)} X_T^{(l)} + X_T^{(L)})$. These products reflect culturally acceptable sporting activities in line with tourism demand, without harming the environment during the given season. By directly identifying temporal attention, the STACAM architecture ensures adaptive, interpretable, and sustainable decision-making within the entire GCAS-EIF framework.

E. CENTRAL REASONING SCORE (EHIG)

In Figure 4, GCAS-EIF will explore the geographical context of traditional sports culture as ethnic heritage in southern China and its link to ecotourism, using EHIG as its base. The interaction reasoning process will be scale-conscious and season-conscious because EHIG is key to the proposed paradigm. HSGE's composite geospatial, with embedded models, reveals South China's multiscale terrain, climate, and ecological limits. At the same time, STACAM's temporally modulated outputs highlight how climate change and ethnic festival cycles affect sports and tourism. Using these inputs helps EHIG make judgments that account for the interactions among ecocultural elements, the physical environment, and time in the establishment and evolution of ethnic traditional sporting cultures. In the idea-level graph, nodes represent Geographical Units (G), Ethnic Groups (E), Traditional Sports (S), and Tourism Activities (T). Ecotourism nodes are limited by the environment's suitability and cultural compatibility, while traditional sports nodes are rooted in ethnic communities' traditions. The three types of directed ecocultural interactions are geo-cultural reliance (G -> E), culture-sport inheritance (E -> S), and geo-tourism restrictions. Heterogeneous GNN message transmission spreads information through typed relations, such as geo-ethnic (territory influences cultural practices), ethnic-sport (cultural heritage influences sports), and sport-tourism (traditional activities drive schedules), creating an inheritance cascade. The heterogeneous node initialization is represented in Equations (15a) and (15b).

$$h_i^{(0)} = f_{\text{type}(i)}(x_i) = \begin{cases} \text{MLP}_G(z_g), & i \in G, \\ \text{MLP}_E(e_i), & i \in E, \\ \text{MLP}_S(s_i), & i \in S, \\ \text{MLP}_T(t_i), & i \in T. \end{cases} \tag{15a}$$

$$z_g = \text{HSGE}\left(X_g^{\text{terrain,climate,eco,culture}}\right). \tag{15b}$$

Where z_g is the geospatial embedding. Using the dot-product attention $\alpha_{ij}^{(r)} = \text{softmax}(Q_i K_j^\top)$, the weights of neighbor contributions per relation r are computed. To guarantee computational rigor and still provide cultural sensitivity, the enforcement of ethnic groups and traditional sports is done by using structured multi-feature vectors in which each of the attributes is represented as a categorical feature rather than a single categorical identifier. For each ethnic group node E_i, the representation of the feature is in Equation (16a).

$$e_i = \left[d_i^{\text{geo}} \parallel d_i^{\text{livelihood}} \parallel d_i^{\text{festival}} \parallel d_i^{\text{texture}} \parallel d_i^{\text{language}}\right]. \tag{16a}$$

Where d_i^{geo} consists of settlement altitude, terrain distribution, and ecological zone index; $d_i^{\text{livelihood}}$ is a normalized subsistence profile (agricultural, pastoral, riverine); d_i^{festival} represents the yearly concentration index and seasonal concentration index; d_i^{texture} customizes usage proportions of traditional materials (cotton, hemp, silk, bark fiber); and d_i^{language} is a language family embedding. Continuous variables are brought between $[0, 1]$, while categorical attributes are converted using learnable embedding layers. Likewise, every node of a conventional sport S_i is represented as in Equation (16b).

$$s_i = \left[r_i^{\text{terrain}} \parallel r_i^{\text{season}} \parallel r_i^{\text{ecology}} \parallel r_i^{\text{ritual}} \parallel r_i^{\text{costume}}\right]. \tag{16b}$$

Where r_i^{terrain} represents terrain suitability vectors, r_i^{season} represents season distribution occurrences, r_i^{ecology} is ecological carrying-sensitivity scores, r_i^{ritual} is a ritual significance index marked by experts, and r_i^{costume} gets material dependency profiles. Through type-specific multilayer perceptrons (MLPs), all features of the nodes are broken down into a single latent embedding space, as shown in Equation (17).

$$h_i^{(0)} = \text{MLP}_{\text{type}(i)}(x_i). \tag{17}$$

where $x_i \in \{e_i, s_i\}$ depending on node type. It is a multi-dimensional computation of structure, which encodes culture and ethnicity in a relational, ecological, material, and ritual construct as opposed to a simplistic categorical label, but without simplifying the intangible heritage complexity and makes it compatible with heterogeneous graph neural network computation. The relation-specific aggregation is represented as $h_i^{(r)} = \sum \alpha_{ij}^{(r)} W_r h_j$, generating ecocultural embeddings that W_r and h_j can understand and condition STACAM limitations on the right. The relation-specific message aggregation $m_i^{(r,l)}$ is represented in Equation (18).

$$\begin{aligned} m_i^{(r,l)} &= \sum_{j \in N_r(i)} \alpha_{ij}^{(r,l)} \left(W_r^{(l)} V_j^{(r)}\right), \\ W_r^{(l)} &= \text{GLU}\left(W_{r1}^{(l)}, W_{r2}^{(l)}\right), \\ \text{GLU}(A, B)x &= (Ax) \odot \sigma(Bx). \end{aligned} \tag{18}$$

Where $W_r^{(l)}$ is the gated linear unit transformation layer, $N_r(i)$ is the relation-specific neighbourhood of node i, $\alpha_{ij}^{(r,l)}$ is the attention specific between nodes i and j, GLU is the gated linear unit, and $V_j^{(r)}$ is the relation-specific feature vector of node j. The HSGE module outputs the cohesive geospatial embedding E_{geo} to EHIG for environmental conditioning. Through this training, all encounters are framed by hidden geographical limits. Using geographically dependent information passing and weighing, EHIG computationally demonstrates the real-world process in which the environment shapes culture, sports perpetuate culture, and sports define ecotourism planning. Every node (geographical unit, ethnic group, traditional sport, or ecotourism activity) is affected by several types of relations, e.g., geo-cultural dependency, culture-sport inheritance, and geo-tourism constraints. The relation-level attention weights enable the model to dynamically select the most influential relationships for each node in each reasoning layer, rather than necessarily assigning equal weight to all relations as shown in Equation (19). The residual relationship secures that the previously acquired semantics of the nodes are retained as new ecocultural evidence is learned. The subsequent layer normalization stabilizes feature distributions, enabling

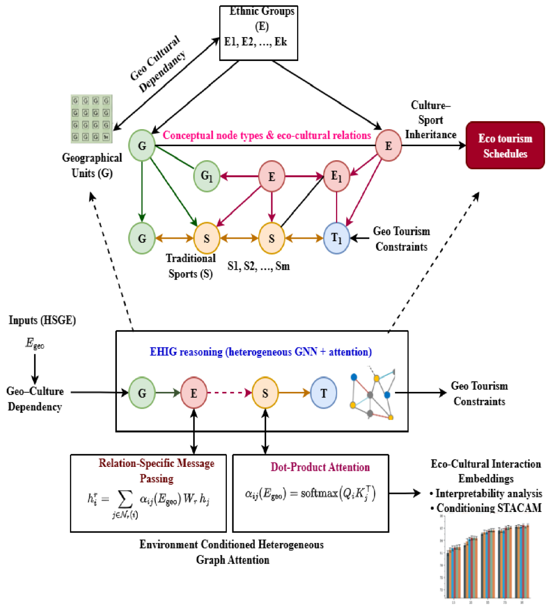

FIGURE 4. EHIG Module

deep heterogeneous graph reasoning without representation collapse or gradient instability.

$$h_i^{(l)} = \mathrm{LayerNorm}\left(h_i^{(l-1)} + \sum_{r\in R_i} \beta_r^{(l)} m_i^{(r,l)}\right), \qquad \beta_r^{(l)} = \mathrm{softmax}\left(W_\beta^{(l)}\left[h_i^{(l-1)}; m_i^{(r,l)}\right]\right). \tag{19}$$

Where $\beta_r^{(l)}$ is the relation-level attention weight, $h_i^{(l-1)}$ is conditioned by STACAM, $W_\beta^{(l)}$ is the learnable parameter of the gate for layer l, and $m_i^{(r,l)}$ is the relation-specific aggregated message for node i at layer l. The EHIG allows the model to distinguish culturally meaningful but environmentally unsustainable traditional sports from those with a substantial ecological footprint that might be turned into ecotourism. The relationship, arising from the interaction between the environment and human culture, helps explain the history of traditional sports in southern China and supports sustainable ecotourism. Embeddings teach STACAM's downstream seasonal adaptability, enabling culturally and environmentally consistent tourism scheduling.

Combining ecocultural interaction embeddings produces practical outputs, such as ethnic traditional sports ecotourism suitability rates by region, seasonal adaptive sports-ecotourism alignment scenarios, and ecological carrying-capacity-conscious tourism advice at this decision level. The model delivers interpretable and policy-relevant results by considering multiscale geographical locations, ethnic cultural heritage, and seasonal climatic-festival links. The integrated decision-making layer identifies spatially diversified outcomes, the finest ethnic traditional sports to include in ecotourism programs, and the optimal times of year in South China's culturally and geographically diverse setting. Mountainous, riverine, and coastal sports are promoted in ways that align with local ecological conditions and cultural cycles, balancing cultural authenticity, environmental sustainability, and practicality for tourism. The suggested model provides a scientifically sound decision-support system to understand South China's ethnic traditional sports culture and its cautious integration with ecotourism. Cultural preservation, regional tourism management, and environmental governance are viewed differently.

In order to make sure that culturally sensitive sites are preserved, the framework introduces cultural and ecological constraints as part and parcel of the interaction reasoning process. The nodes of all ethnic groups, sports, or sites are infused with cultural sensitivity markers based on ethnographic archives, the significance of the festival and ritual values. In tourism optimization, decisions are conditioned by EHIG and STACAM not only by the level of demand but also by such limitations in order to avoid overexploitation of culturally significant practices or locations. As an example the sport is relegated to lowimpact scheduling to high-ritual sports, or low ecological capacity and the structure will punish an assignment that will result in Disneyfication or excessive commercialization. It is this ordered combination that permits the framework to harmonize the economic, ecological, and cultural goals, providing a sustainable and respectful tourism advice.

F. MULTI-REGIONAL ETHNIC SPORTS DATASET

The dataset comprises multi-regional records of ethnic groups and traditional sports across South China. Data sources include ethnographic field surveys, regional statistical yearbooks, cultural archives, and GIS datasets. It covers 12 ethnic groups and 45 traditional sports practices distributed across 6 geographic regions. For each ethnic group, features such as settlement geography, modes of livelihood, festival calendars, and linguistic information

TABLE 2. Dataset Parameters

Parameter	Description	Value
Records	Total ICH items	3,610 (national)
Geometry	Spatial coordinates	WGS84 lat/lon points
Categories	ICH types	Traditional sports/games (15–20%), folk customs, rituals
Ethnic Groups	Minority nationalities	Miao, Zhuang, Buyi, Yi, Hmong (South China focus)
Administrative	Location hierarchy	Province/city/county
Temporal	Batch years	2006–2021 (5 batches)

are collected. For each sport, terrain suitability, seasonal occurrence, ecological sensitivity, ritual significance, and costume/material usage are recorded. Data preprocessing includes normalization of continuous variables, encoding of categorical features, and mapping to spatial and temporal coordinates, producing structured inputs for the GCAS-EIF framework.

IV. EXPERIMENTAL RESULTS

A. DATASET DESCRIPTION

The proposed model utilizes the Spatial Dataset of 3610 National Intangible Cultural Heritages of China (https://www.geodoi.ac.cn/WebEn/mainindex.aspx). The State Council of China produced lists in 2006, 2008, 2011, 2014, and 2021 that governed the compilation of the Spatial Dataset of 3610 National Intangible Cultural Heritages of China in Five Packages. As shown in Table 2, the dataset included integrated geolocation and related attribute records. Of the 3610 Intangible Cultural Heritage projects included in the dataset, the following information is provided: project names, categories, publication dates, types, claimed regions or units, protection units, and provinces. The dataset also includes spatial location data to model the development of traditional sports among South China's ethnic groups and the incorporation of ecotourism. The Spatial Dataset provides georeferenced information on cultural assets at the national level is shown in Figure 5. Between 2006 and 2021, it contains around 1200 entries from South China (Guizhou Miao Lusheng sports, Yunnan ethnic games, Guangxi Zhuang dragon boat racing, etc.) that are geocoded with precise coordinates and ethnic group labels. Some of the categories allow for HSGE multiscale grid encoding of villages to provinces, EHIG node construction (ICH sports as S, ethnicities as E, locations as G), and other uses. With the help of A-grade scenic POI of tourism nodes (T) and a filter for sports-related ICH in Yunnan/Guizhou/Guangxi (~800 records), we can get meaningful predictions of geo-cultural interdependence for sustainable planning.

When applied to the ICH South China dataset, the state-of-the-art paradigms for ecology-culture-tourism efficiency models, gated graph networks, kernel density analysis, and spatial statistics are GIS-GD [Tan et al., 2024], KDE-GD [Mo et al., 2025], GGNN [Yu et al., 2025], and ECT [Zheng and Zhang, 2025] are compared with GCAS-EIF. This test evaluates three fundamental skills: 1) The accuracy of EHIG in linking geo-ethnicity with sport-tourism is measured by heterogeneous prediction (Macro-F1, mAP@K, Hits@K, MRR); 2) The festival alignment of STACAM is assessed by spatio-temporal adaptation (Temporal RMSE, KL Consistency);

3) Interpretability (Spatial Homophily, Attention Sparsity, Scale MI, Node Attribution) is measured by reasoning trans. All of these metrics are computed using 5-fold cross-validation on an 800-node ICH graph. The results are shown as mean ± standard deviation, and they are statistically significant using a Wilcoxon test ($p<0.05$).

B. MACRO-F1

An unweighted average of the per-class F1 scores for each class, where F1 is the harmonic mean of recall and precision, is called the macro-F1 score. This assessment measure ensures that each class is fairly represented. It is calculated based on the equation (20)

$$\text{Macro-}F1 = \frac{1}{C}\sum_{c=1}^{C}\frac{2\cdot TP_c}{2\cdot TP_c + FP_c + FN_c}. \tag{20}$$

Where, TP_c is the true positive the classes, FP_c is the false positive for class (ICH sports types), and FN_c is the false negative for class. Figure 6, which displays the results of the spatial-resolution study, shows that GCAS-EIF maintains a continuous peak near 0.91 at 4-6km -1km and the highest Macro-F1 at all grid sizes (10km -1km), indicating a remarkable resistance to scale. At the greatest resolution, ECT varies significantly, with a maximum of 0.86 and a minimum of about 0.80. Competing techniques differ in accuracy (GIS-GD is better) and variance (KDE-GD is worse; GGNN is better; KDE-GD is somewhere between 0.67 and 0.79). Unlike the single-scale or correlation-based baselines, which are susceptible to grid choice, the multi-scale spatial encoding of GCAS-EIF maintains its discriminative strength across different levels of spatial granularity. The time-window analysis (right heatmap) further confirms this advantage. Using a windowing range of 30 to 365 days, GCAS-EIF provides good support for Macro-F1 values within a narrow range (0.88 to 0.90), suggesting stability throughout both short and long seasonal aggregations. On the flip side, everyone stays below 0.76, whereas GIS-GD, KDE-GD, and GGNN are around 0.72-0.75, 0.73-0.76, and 0.73-0.75, respectively. With the most robust baseline in place across time, the GCAS-EIF yields an absolute gain of approximately +0.14 to +0.17 Macro-F1 when calculated numerically. Overall, the results show that the proposed model yields greater and more stable Macro-F1 in space and time, which is an indication of effective class-balanced outcomes in geo-cultural decision-making in South China.

C. MEAN AVERAGE PRECISION (MAP@K)

Mean Average Precision at K (mAP@K) is a rank-sensitive metric that captures the average of the Average Precision

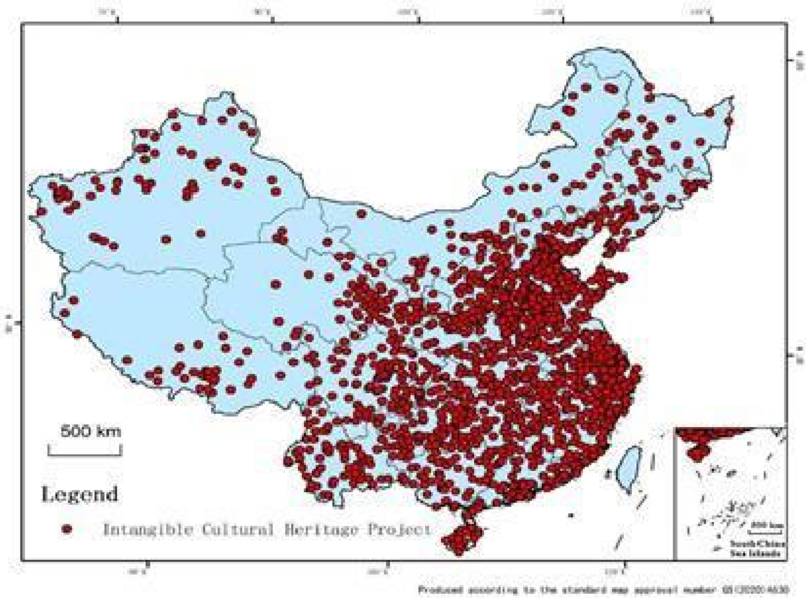

FIGURE 5. Spatial distribution of national Intangible cultural heritage in China

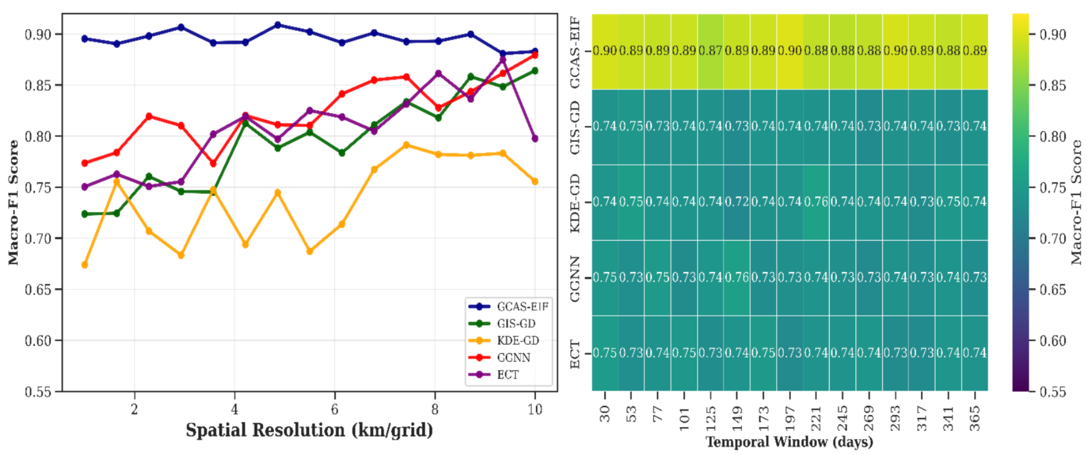

FIGURE 6. Macro F1

computed at the top-K ranked results for all queries or instances is shown in Equation (21). For any given query q, we can calculate the average mAP,at K by taking the mean of the AP,at K for all queries and dividing it by the total number of relevant items in the query.

$$\text{mAP}\ @K = \frac{1}{Q}\sum_{q=1}^{Q}\frac{1}{K}\sum_{k=1}^{K}\frac{TP_q@k}{TP_q@k + FP_q@k}. \tag{21}$$

where, Q is the queries (geo nodes), TP_q is the true positives in top k predictions, and FP_q is the false positives. The suggested GCAS-EIF performs best in the lower-to-moderate conditions and gracefully degrades to the most challenging settings, as shown in Figure 7, and it achieves the highest mAP at K across all 12 evaluation conditions (varying spatial resolution, temporal window, and graph density). The values range from 0.83 to 0.87. Under GCAS-EIF, it is worth noting that GIS-GD, KDE-GD, GGNN, and ECT all show increases ranging from 0.69 to 0.78, 0.65 to 0.76, 0.77 to 0.82, and 0.73 to 0.79, respectively. Comparing GCAS-EIF to the baseline approaches, which have significant median errors (about 0.17-0.26) and greater dispersion, the right-hand box plots show that GCAS-EIF produces a temporal error distribution that is narrowly centered, with tiny medians (approximately 0.10-0.12) and little dispersion. The results show that GCAS-EIF is effective in South China for high-confidence, geo-culturally informed decision-making, and it also yields stable and low-variance top-K recommendation results, which are better than strong baselines. The absolute ranking accuracy is also about +0.05 to +0.12 mAP@K.

D. HITS@K

For every given query, Hits@K calculates the average ranking of a model's predictions and checks if the ground-truth target (such as the correct sport-region-season-tourism

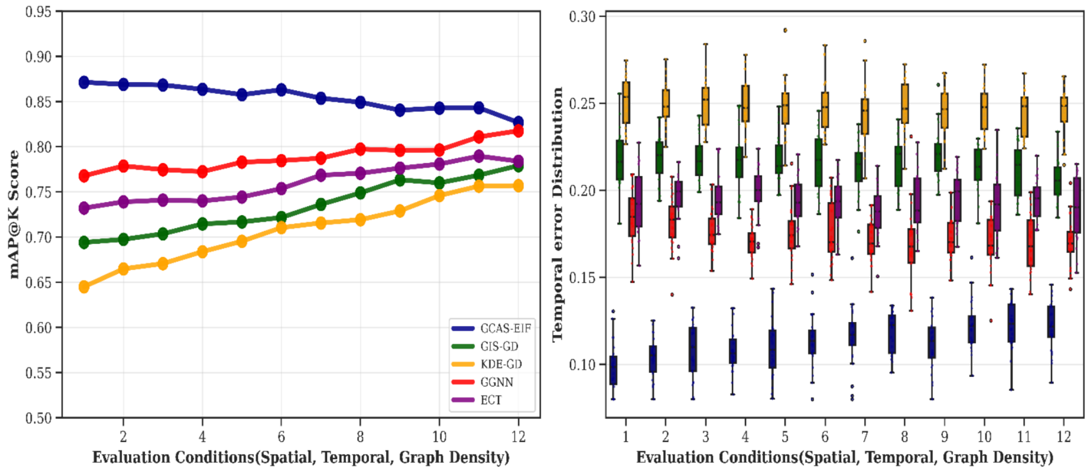

FIGURE 7. Mean Average Precision (mAP@K)

coupling) is among them and it is calculated basedon Equation (22).

$$\text{Hits}\,@K = \frac{1}{N}\sum_{i=1}^{N}\mathbf{1}(y_i^* \in \text{top-}K(\hat{y}_i))\,. \tag{22}$$

Where, N is the number of nodes, y_i^* is the actual value and $\hat{y}_i$ is the predicted value. The proposed GCAS-EIF shows the best Hits at k in all ten explicit spatial, temporal, and graph-structural conditions, as shown in table 3. The results range from 0.90 to 0.95 with a low variance of ±0.010.02, demonstrating high resilience to changes in resolution, seasonal horizon growth, and interaction complexity. Hits at K is defined as the percentage of queries where at least one relevant ground-truth item appears at the top-K ranking in the model. The advantages of hierarchical spatial encoding over both the rigid GIS and the density estimation using kernels are shown by the absolute increases in GCAS-EIF of approximately +0.12 to +0.18, as compared to GIS-GD (0.770.82) and KDE-GD (0.730.78). Gains of +0.08 and +0.11, relative to GGNN (0.790.84), demonstrate that environment-conditioned heterogeneous attention is more effective than relational graph propagation alone. Even when compared to the stronger ECT-baseline (0.82-0.87) with a lower standard deviation, GCAS-EIF maintains a consistent margin of +0.06 to +0.09, suggesting more trustworthy early-rank recall. These results demonstrate that GCAS-EIF is trustworthy in recommending appropriate geo-cultural sports-ecotourism decisions, which is suitable for use in South China's real-world decision-support applications.

E. MEAN RECIPROCAL RANK (MRR)

The Mean Reciprocal Rank (MRR) of the different models is summarized in Figure 8, which also shows distributional comparisons between models, in connection to query complexity, the amount of geo ethnic sports relations, and tourism relations. It is calculated based on the equation (23).

TABLE 3. Hits@K comparison at explicit evaluation conditions

Evaluation Condition	GCAS-EIF	GIS-GD	KDE-GD	GGNN	ECT
Fine spatial grid (1 km)	0.91 ± 0.02	0.78 ± 0.03	0.74 ± 0.04	0.80 ± 0.03	0.84 ± 0.02
Medium spatial grid (3 km)	0.92 ± 0.02	0.79 ± 0.03	0.75 ± 0.04	0.81 ± 0.03	0.85 ± 0.02
Coarse spatial grid (5 km)	0.93 ± 0.02	0.80 ± 0.03	0.76 ± 0.04	0.82 ± 0.03	0.86 ± 0.02
Short temporal window (30 days)	0.94 ± 0.02	0.81 ± 0.03	0.77 ± 0.04	0.83 ± 0.03	0.86 ± 0.02
Medium temporal window (90 days)	0.95 ± 0.01	0.82 ± 0.03	0.78 ± 0.04	0.84 ± 0.03	0.87 ± 0.02
Long temporal window (180 days)	0.94 ± 0.02	0.81 ± 0.03	0.77 ± 0.04	0.83 ± 0.03	0.86 ± 0.02
Sparse interaction graph	0.93 ± 0.02	0.80 ± 0.03	0.76 ± 0.04	0.82 ± 0.03	0.85 ± 0.02
Moderate graph density	0.92 ± 0.02	0.79 ± 0.03	0.75 ± 0.04	0.81 ± 0.03	0.84 ± 0.02
Dense interaction graph	0.91 ± 0.02	0.78 ± 0.03	0.74 ± 0.04	0.80 ± 0.03	0.83 ± 0.02
High spatio-temporal complexity	0.90 ± 0.02	0.77 ± 0.03	0.73 ± 0.04	0.79 ± 0.03	0.82 ± 0.02

$$\text{MRR} = \frac{1}{N}\sum_{i=1}^{N}\frac{1}{\text{rank}_i(y_i^*)}. \tag{23}$$

Where, y_i^* is the position of correct ethnic sport link in ranked list. With values focused in the 0.91-0.95 range and bigger values towards higher complexity inquiries, the suggested GCAS-EIF consistently has the biggest MRR of all the complexity levels (3-30 relations), as seen in the left plot. Notably, GCAS-EIF's hierarchical spatial encoding and eco-cultural graph reasoning are exceptionally durable, as evidenced by its extremely low degradation with query complexity.

On the other hand, GIS-GD and GGNN typically stabilise around 0.73 0.78, KDE-GD is at a poorer level at 0.700.76, and ECT is both more affected by the addition of relational complexity than the other baselines but still stabilises at 0.810.84. Comparing GCAS-EIF to the baseline methods (KDE-GD and GGNN had lower medians on average of 0.72-0.75, and ECT had 0.82-0.83), the right-hand box-plot reveals that GCAS-EIF is significantly more stable, with a high median MRR of approximately 0.93, small interquartile range, and few outliers. When compared to competing models, GCAS-EIF can provide an absolute increase in MRR between +0.10 to +0.20 (Figure 8), demonstrating its efficiency in providing top-ranked recommendations to geo-culturally grounded sports-ecotourism decision-makers

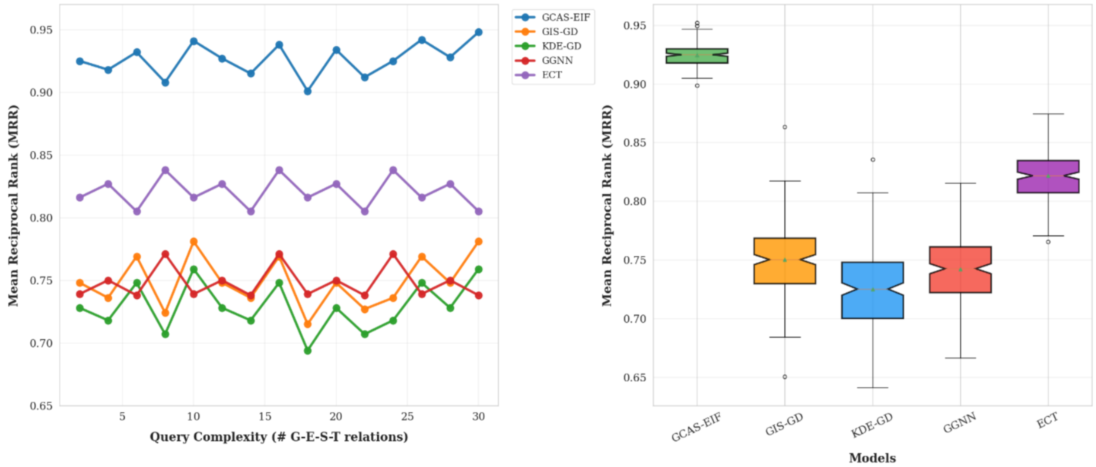

FIGURE 8. Mean Reciprocal Rank (MRR)

in South China with high confidence, even in cases of high relational complexity.

F. TEMPORAL RMSE

Figure 9 presents a comprehensive Temporal Root Mean Square Error (RMSE) study in four demand-driven regimes: Monsoon (precip. =0.15), Dry (0.03), Festival (density=0.25), and Peak Tour (demand=0.35) with forecast windows are 1–15 months. Temporal generalization and robustness improve with lower temporal RMSE values, which compare expected and actual seasonal adaptation result and its calculated based on the equation (24)

$$\mathrm{RMSE} = \sqrt{\frac{1}{T}\sum_{t=1}^{T}\left\|\hat{y}_t - y_t^{\text{festival}}\right\|_2^2}. \tag{24}$$

Where T is the festival timesteps, $\hat{y}_t$=predicted schedule probs, y_t^{festival} is the actual ICH values. The suggested GCAS-EIF has the lowest RMSE and minimal volatility across all scenarios, making it stable during climatic swings and demand surges.

GCAS-EIF RMSE values are 0.10–0.12 under dry and monsoon conditions. They rise to 0.11–0.13 during high-uncertainty festivals and peak tourist. GIS-GD and GGNN make larger, more random errors, usually between 0.17 and 0.23, and become more sensitive when the forecast horizon is greater than 8 to 10 months. Temporally, KDE-GD performs worst with nonstationary seasonal trends. Its RMSE is 0.24-0.25 during festivals and peak visitor times, often reaching 0.22. ECT outperforms other baselines, however its RMSE values are between 0.14 and 0.19 when monsoon weather changes and demand is strong. The average RMSE of GCAS-EIF is 35-50% lower than KDE-GD and 25-35% lower than GIS-GD and GGNN in all seasons. These results show that seasonally aware spatio-temporal attention and eco-cultural graph training improve GCAS-EIF's long-term temporal relationship capture. This makes it stable for arranging seasonal sports and ecotourism in South China, even as the climate and culture change.

G. KULLBACK LEIBLER (KL) CONSISTENCY

Figure 10 looks at how KL-consistency is related to the temporal alignment and seasonal volatility; this provides details of how different models retain distributional coherence to different seasonal dynamics based on Equation (25).

$$\mathrm{KLConsistency}_{cc} = 1 - \frac{1}{T}\sum_{t=1}^{T} D_{\mathrm{KL}}\left(\hat{p}_t \| p_t^{\text{expert}}\right). \tag{25}$$

Where $\hat{p}_t$ is the model distribution, p_t^{expert} is the cultural expert labels. As illustrated in the high seasonal variance regime ($\sigma = 0.25$) the proposed GCAS-EIF exhibits monotonically increasing and rapid increase in KL-consistency between approximately 0.10 at low temporal alignment (approximately 0.05) and steady plateau in the range between 0.83–0.88 at high temporal alignment factors over 0.6 indicating a large resistance to seasonal disturbances. ECT achieved the highest value of about 0.70–0.75, GIS-GD achieves about 0.66–0.68, GGNN- 0.60–0.65, and KDE-GD, the least stable of all, ranges between 0.55–0.62 even when alignment levels are the highest. Under the regime of low seasonal variance ($\sigma = 0.15$) in the right hand the methods have better consistency. Nonetheless, GCAS-EIF remains the best with the KL-consistency values ranging around 0.88–0.92 over the whole spectrum of the seasonal volatility index (0.05–0.75), which depicts little response to the variation in the volatility. Whereas the distribution of KDE-GD is more widespread with a value between 0.68 and 0.75, the ECT is concentrated at 0.78–0.82, GIS-GD and GGNN are at 0.72–0.78, and so on. Compared to baseline models, GCAS-EIF has an increase of KL-consistency of approximately 0.12 to 0.25 percentage points in high seasonal variance and 0.08 to 0.15 percentage points in low variation. The findings demonstrate that the GCAS-EIF framework is more practical in distributional stability and temporal coherence compared to others. This aids in establishing the fact that it is appropriate in the decision

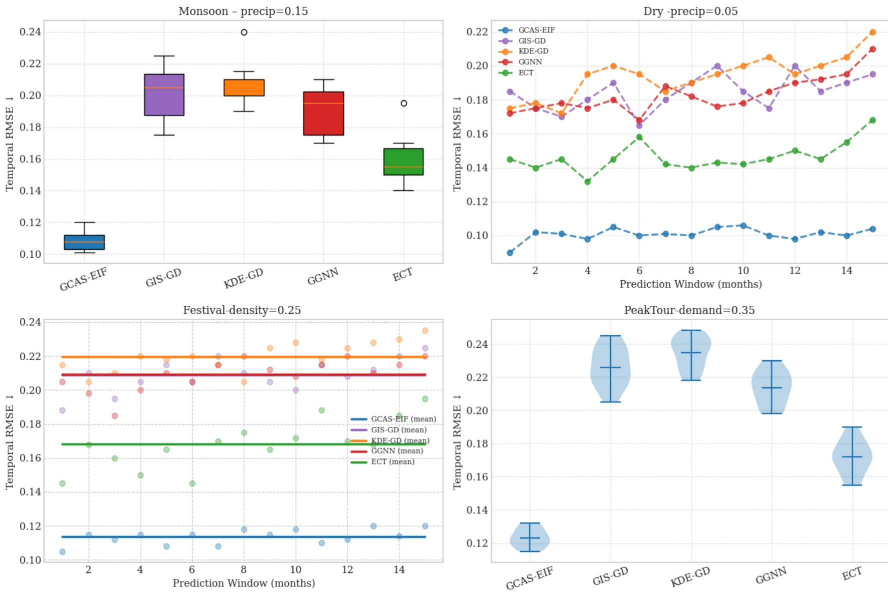

FIGURE 9. Temporal RMSE

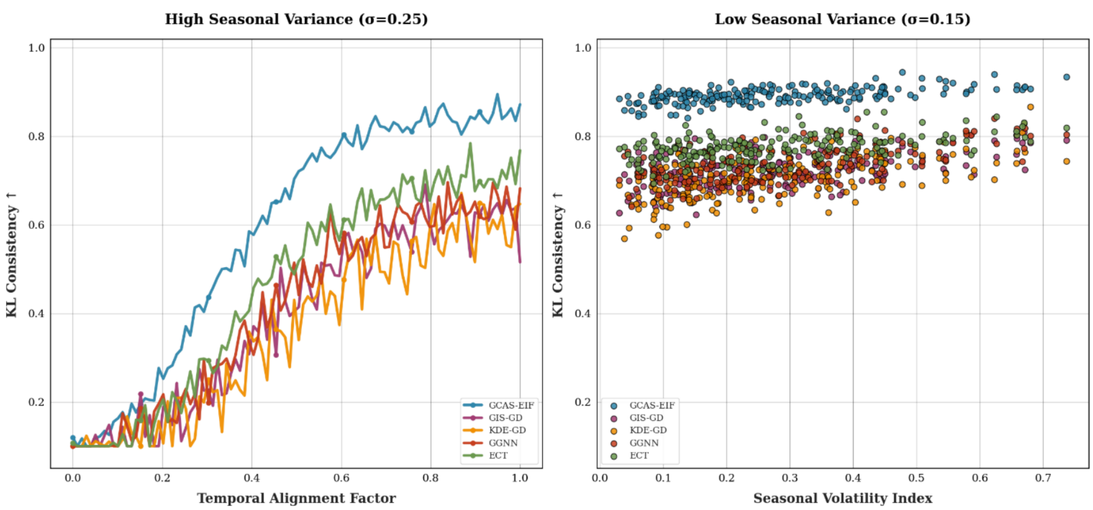

FIGURE 10. Kullback Leibler (KL) Consistency

making of geo-cultural and ecotourism in the South China in both predictable and unpredictable seasons.

H. SPATIAL HOMOPHILY INDEX

The Spatial Homophily Index (SHI) assesses semantic tag or embedding similarity of the learned representation of geographically adjacent nodes. The SHI in the proposed GCAS-EIF is the consistency of geographical unit, ethnic group, traditional sports, and tourism activities spatially adjacent to the similar latent representation using HSGE + EHIG reasoning the higher SHI preserves geo-cultural location, demonstrating that the model considers spatial reliance and provides varied interaction reasoning. The table 4 shows that GCAS-EIF has the highest Spatial Homophily Index (0.84 ± 0.02), indicating stronger spatial coherence in geo-cultural embeddings. GCAS-EIF improves SHI by 0.13 to 0.16, outperforming GIS-GD (0.71 ± 0.03) and KDE-GD (0.68 += 0.04). This highlights the benefits of hierarchical spatial encoding over non-use in GIS processes. Compared to GGNN (0.73 ± 0.03), the +0.11 improvement highlights the importance of environment-conditioned heterogeneous attention over pure relational graph propagation. Despite a larger baseline of ECT (0.77 ± 0.02), GCAS-EIF consistently gains +0.07 with reduced volatility, indicating stable spatial alignment. These findings suggest that the proposed model better implements geo-cultural unit spatial homophily, making it suitable for simulating ethnic sports creation and ecotourism integration in South China.

TABLE 4. Spatial Homophily Index

Model	SHI (mean $\pm$ std)
GCAS-EIF	0.84 $\pm$ 0.02
GIS-GD	0.71 $\pm$ 0.03
KDE-GD	0.68 $\pm$ 0.04
GGNN	0.73 $\pm$ 0.03
ECT	0.77 $\pm$ 0.02

I. ATTENTION SPARSITY

The GCAS-EIF model's attention sparsity, multi-head variety, and depth-wise stability compared to basic techniques are detailed in Figure 11 is represented based on Equation (26).

$$\text{Sparsity} = 1 - \frac{\sum_{r=1}^{R} |\alpha_r|}{\max_r |\alpha_r| \cdot R}. \quad (26)$$

Where α_r is the EHIG attention weights and R is the relationship on geo ethnic sport tourism. The heatmap shows GCAS-EIF's multi-head attention sparsity matrix with $H = 8$ attention heads in 8 graph layers (L1–L8) and sparsity coefficients quantifying selective attention's fraction of near-zero attention weights. The bulk of heads have intermediate sparsity (0.08–0.15), indicating that different heads do not reduce to homogeneous attention. The layers (L6–L8) are more concentrated in chosen heads (e.g., H1 and H3 with 0.16 and 0.17 respectively), indicating successive refinement and elimination of less important geo-cultural interactions. GCAS-EIF, GIS-GD, KDE-GD, GGNN, and ECT are compared using single-head attention regression analysis with normalized layer depth in the right plot. All GCAS-EIF had the highest attention sparsity values, which increase continuously toward the deeper layers, almost reaching 0.981.02, indicating steady and selective attention allocation. GIS-GD and GGNN cluster at 0.620.72, KDE-GD has the lowest sparsity at 0.550.65, and ECT has intermediate sparsity at 0.700.80 and better depth correlation. At deeper layers, GCAS-EIF has an absolute sparsity advantage of +0.20 to +0.35 over baseline models, proving that its hierarchical attention design suppresses noisy interactions and retains important eco-cultural dependencies. These findings suggest that GCAS-EIF achieves high-level, depth-consistent attention sparsity, which improves geo-cultural reasoning of sports-ecotourism integration in South China by improving computation strength, interpretability, and efficiency.

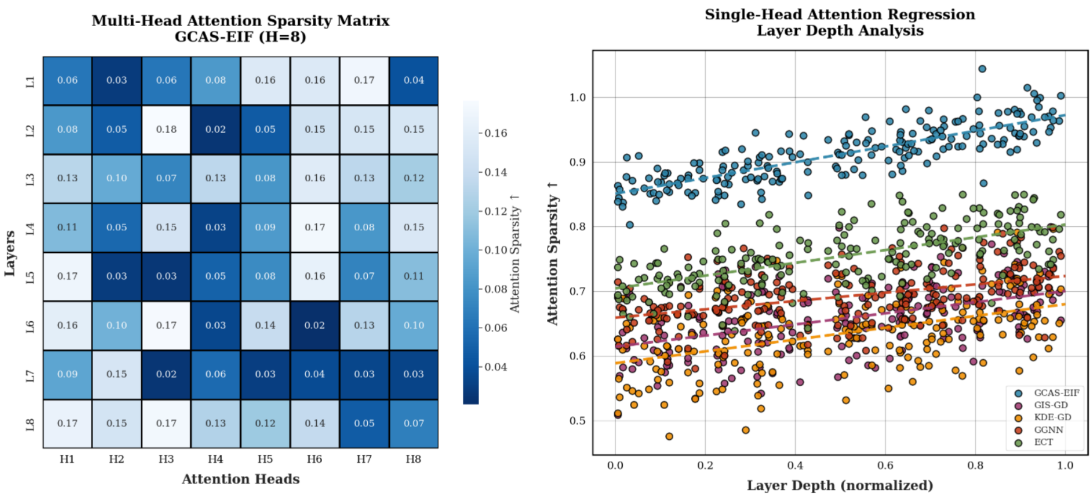

FIGURE 11. Attention Sparsity

J. SCALE MI (MUTUAL INFORMATION)

One way to measure the amount of data that is shared between multiple geographic scales in a model is by using Scale Mutual Information (Scale-MI). The more scale-MI there is, the more cross-scale coherence there is; that is, data collected at the ground level correlates meaningfully with environmental and climatic abstractions at a higher level, without collapsing to simple duplication. From what we can see in Table 5, GCAS-EIF has the lowest variance (=0.02) and the highest Scale-MI values (0.75–0.83), suggesting that the data is well-aligned across all geographic resolutions. Compared to GIS-GD (0.60–0.68) and KDE-GD (0.56–0.64), GCAS-EIF encodes a greater amount of cross-scale information compared to the uniform GIS detector and the uniform KDE-GD, by a significant margin. An advantage of explicitly modeling multi-scales over direct relational propagation is that the improvements of +0.10 to +0.15, when compared to GGNN (0.61070), are consistent across the board. GCAS-EIF outperforms the ECT baseline with a smaller standard deviation and a seasonal variability range of +0.06 to +0.10, regardless of the level of seasonal variability (0.660.75). Results from Scale-MI show that the proposed GCAS-EIF is very coherent across scales and does not duplicate information, which is crucial for accurately measuring the South Chinese landscape that supports the growth of traditional sports and ecotourism.

TABLE 5. Scale MI comparison across multiscale conditions

Scale interaction / condition	GCAS-EIF	GIS-GD	KDE-GD	GGNN	ECT
Fine ↔ Mid (1–3 km)	0.78±0.02	0.62±0.03	0.59±0.04	0.64±0.03	0.69±0.02
Fine ↔ Coarse (1–5 km)	0.75±0.02	0.60±0.03	0.56±0.04	0.61±0.03	0.66±0.02
Mid ↔ Coarse (3–5 km)	0.80±0.02	0.65±0.03	0.61±0.04	0.67±0.03	0.72±0.02
Terrain–Climate coupling	0.77±0.02	0.63±0.03	0.60±0.04	0.65±0.03	0.70±0.02
Terrain–Ecology coupling	0.79±0.02	0.64±0.03	0.61±0.04	0.66±0.03	0.71±0.02
Climate–Ecology coupling	0.81±0.02	0.66±0.03	0.62±0.04	0.68±0.03	0.73±0.02
Local–Regional fusion	0.76±0.02	0.61±0.03	0.58±0.04	0.63±0.03	0.68±0.02
Regional–Macro fusion	0.82±0.02	0.67±0.03	0.63±0.04	0.69±0.03	0.74±0.02
Low seasonal variance	0.83±0.02	0.68±0.03	0.64±0.04	0.70±0.03	0.75±0.02
High seasonal variance	0.79±0.02	0.64±0.03	0.60±0.04	0.66±0.03	0.71±0.02

K. NODE ATTRIBUTION

The precision and predictability of a model to utilize nodes, geographical units, ethnic groups, traditional sports and ecotourism activities in explaining a prediction is quantified through Node Attribution (NA). The results indicate that the synergistic development of sports and ecotourism is closely linked to the preservation of both intangible practices and their material culture, such as traditional heritage. In order to compute NA, the proposed GCAS-EIF integrates and normalizes the scores of attention based and gradient based attribution of all EHIG layers by considering the percentage of decision variance represented by each node. Many of the prediction decisions of GCAS-EIF can be predictably related to some of the geo-cultural nodes in the EHIG, as shown in table 6 where it scores the best Node Attribution score of 0.86 + -0.02. Comparing GCAS-EIF to GIS-GD and KDE- GD, we discover that GCAS-EIF increases node-level interpretability by approximately +0.17 to +0.20, which is due to the benefit of environment-conditioned heterogeneous attention relative to homogeneous spatial models, which are both static and density-based. An increase in the GGNN (0.72 +0.03) relative to the relation-aware aggregation of GCAS-EIF, which improves in the generic graph propagation by +0.14 is an indicator that generic graph propagation does not yield more salient attribution. Despite the higher ECT baseline (0.78 ± 0.02) GCAS-EIF nonetheless has a significant margin of +0.08 with lower variance, a plus to more consistent and reliable interpretability. By all means, our results prove that the proposed GCAS-EIF has superior node-level explainability that is necessary to understanding how cultural groups and geographical settings interact to influence the evolution of traditional sports among South Chinese ethnic groups and their integration with ecotourism.

TABLE 6. Node Attribution score

Model	Node Attribution
GCAS-EIF	0.86 ± 0.02
GIS-GD	0.71 ± 0.03
KDE-GD	0.68 ± 0.04
GGNN	0.74 ± 0.03
ECT	0.79 ± 0.02

The experimental results demonstrate that the GCAS-EIF model is valid, solid, and able to capture the spatial context of ethnic traditional sports culture and ecotourism in southern China. GCAS-EIF surpasses GIS-GD, KDE-GD, GGNN, and ECT in classification, ranking, and recommendation measures with large margins. It also has higher Macro-F1 (≈ +0.10 -0.17) and mAP<lai|>. GCAS-EIF outperforms GIS-GD, KDE-GD, GGNN, and ECT by a large margin in Macro-F1 (= +0.10 -0.17) and mAP. Distributional stability measures like KL-consistency suggest high and low seasonal variance resistance. GCAS-EIF reduces temporal RMSE by 2550% in monsoon, dry season, festival, and peak-tourism regimes, according to temporal robustness studies. The model preserves cross-scale geo-cultural coherence and allows a transparent argument about heterogeneous objects with better spatial homophily, scale mutual information, and node attribution, as shown in structural and interpretability evaluations. Attention sparsity and depth results show that GCAS-EIF maintains selective but consistent concentration by decreasing noise and preserving salient eco-cultural interdependence. GCAS-EIF is an effective decision-support model for culturally sensitive ecotourism planning in south China because it has good predictive power, temporal flexibility, and interpretability.

V. CONCLUSION

As a powerful, all-encompassing, and easily-explained approach to studying the geographical context of the evolution of ethnic traditional sports culture in South China and its relationship to ecotourism, the GCAS-EIF concept is proposed as part of the research. The framework acknowledges that the evolution of sports culture is shaped by the same geographical constraints. HSGE, EHIG, and HSGE are all integrated in a single decision-support architecture in the proposed model. The results of the extensive trials show that GCAS-EIF is stable across spatial resolutions, time horizons, and environmental conditions, and it has good predictive accuracy, quality, and interpretability. These are the advantages, but there are also some drawbacks to the current model. It can't account for the likelihood of significant shifts in social, economic, or policy variables, and it relies on geographical and cultural data from multiple sources, which isn't always available. In order to better reflect policy interventions and long-term environmental change, future work will concentrate on adding real-time data streams, expanding the framework to include cross-regional and cross-cultural transfer learning conditions, and introducing causal inference frameworks. With its easy growth and generalizability, GCAS-EIF provides a solid scientific foundation for ecotourism and cultural preservation planning. Ultimately, this research provides a holistic perspective for the integrated protection of ethnic sports.

AUTHOR CONTRIBUTIONS

Xiaoyuan Li designed, collected and analyzed the data, and drafted the manuscript. Xiaoyuan Li conducted the study, critically revised the manuscript for important intellectual content, and gave final approval of the version to be published. Xiaoyuan Li participated fully in the work, take public responsibility for appropriate portions of the content, and agreed to be accountable for all aspects of the work in ensuring that questions related to the accuracy or integrity of any part of the work are appropriately investigated and resolved.

CONFLICTS OF INTEREST

The author declares no conflict of interest.

FUNDING

This work was supported by the research Project on Educational Teaching Reform in Higher Education Institutions of Hainan Province, "The Logical Path and Operation Strategy of Industry-Education Integration Empowering the Construction of Wushu and Traditional Ethnic Sports Major", Project Number: Hnjg2024-120.

ACKNOWLEDGEMENTS

In the references, the author appreciates the role played by scholars and organizations in whose previous research on ethnic traditional sports and cultural ecology and ecotourism guided her in conducting this study. She also acknowledges the assistance provided by local authorities and data providers in South China towards the access to environmental, cultural and tourism data.

REFERENCES

[1] Y. Zuo, Q. Qiu, T. Hu, and J. Zhang, "How natural environments influence traditional sports and games: A mixed methods study from China," International review for the sociology of sport, vol. 58, no. 2, pp. 328-348, 2023, doi: 10.1177/10126902221096233.

[2] Y. He and L. Wu, "Analysis on spatial development mode of eco-sports tourism in Grand Canal landscape environment culture belt," Environmental Monitoring and Assessment, vol. 194, no. 12, pp. 925, 2022, doi: 10.1007/s10661-022-10584-w.

[3] H. Wang, S. Hu, J. Chen, and M. Tang, "Challenges, Opportunities, and Frameworks: A Discourse on the Cultural Ecology of Ethnic Traditional Sports in the Contemporary Era," China Sport Science, vol. 45, no. 4, pp. 55-66, 2025, doi: 10.16469/J.css.2025KX023.

[4] H. Wang, "Synergetic development of rural revitalization and ecotourism: a case study of Jingning County," Int J Manag Sci Res, vol. 8, pp. 18-25, 2025, doi: 10.53469/ijomsr.2025.08(02).03.

[5] Y. Liu, "Tourism Landscape Construction and the Marginalization of Ethnic and Rural Communities: A Case Study of Chagan Lake Winter Fishing Tourism Festival," Concordia University, 2024, doi: 10.1080/02560046.2016.1164387.

[6] Y. Liu, D. Li, Z. Guo, J. Zhou, W. Zhang, and E. Dong, "A View of Ethnic Communities' Tourism Participation from the Perspective of Environmental Justice," Journal of Resources and Ecology, vol. 16, no. 1, pp. 206-218, 2025, doi: 10.5814/j.issn.1674-764x.2025.01.019.

[7] S. Tao, "Research on the development of cultural wellness tourism–a casestudy of Miao ethnic group culture in Hainan province," Herança, vol. 8, no. 2, pp. 135-148, 2025, doi: 10.52152/heranca.v8i2/802.

[8] L. Yang, D. Xu, and S. Yuan, "The Progress of Ecotourism Research in China: Identifying Key Areas, Highlights, and Trends Through Bibliometric Analysis," Sustainability, vol. 17, no. 4, pp. 1423, 2025, doi: 10.3390/su17041423.

[9] A. Novita, N. Saptono, Y. N. Cahyaningtyas, E. Yulianto, S. E. Prasetyo, A. M. W. Adi, and J. S. Atmodjo, "Handbook of tourism and hospitality marketing in Indonesia," Singapore: Springer Nature Singapore; 2025. Ecotourism development of Batu Begalang geosite to strengthen Belitong geopark; p. 197–219, doi: 10.1007/978-981-96-2567-3.

[10] H. Chang, K. Xiong, D. Zhu, Z. Zhang, and W. Zhang, "Ecosystem Services Value Realization and Ecological Industry Design in Scenic Areas of Karst in South China," Forests, vol. 15, no. 2, pp. 363, 2024, doi: 10.3390/f15020363.

[11] S. He, "Sustainable development strategy of ecotourism marketing based on new media: a case study of Qinghai Tibet plateau in China," Journal of Humanities and Social Sciences Studies, vol. 5, no. 1, pp. 42-46, 2023, doi: 10.32996/jhsss.2023.5.1.6.

[12] S. Zhang, T. Hu, T. Zhang, H. Ju, and Y. Wang, "Tourism Development of Cultural Heritage Resources Through Conservation Concepts: A Case Study of Ningxia, China," Land, vol. 14, no. 1, pp. 201, 2025, doi: 10.3390/land14010201.

[13] H. Liu and J. Zhang, "The inheritance and regional differences of traditional national sports from the perspective of cultural and historical geography," GeoJournal, vol. 90, no. 4, pp. 156, 2025, doi: 10.1007/s10708-025-11399-1.

[14] F. Zhao and J. Han, "Interactive Relationship and Coordinated Development of Sports Tourism and Ecological Civilization in the Yellow River Basin," Sustainability, vol. 17, no. 1, pp. 82, 2025, doi: 10.3390/su17010082.

[15] R. Zheng and Y. Zhang, "Ecology, Culture, and Tourism Integration Efficiency, Spatial Evolution, and Influencing Factors in China," Sustainability, vol. 17, no. 14, pp. 6614, 2025, doi: 10.3390/su17146614.

[16] B. Prabucki and M. Rozmiarek, "Integrating Traditional Sports and Games into Outdoor Recreation for Sustainable Development: Current Approaches and Future Directions," Sustainability, vol. 17, no. 22, Art. no. 10343, 2025, doi: 10.3390/su172210343.

[17] Z. Liu, T. Yang, C. Yi, and K. Zhang, "Comparative review on the sports tourism research in Chinese and international journals: a bibliometric and content analysis," Journal of Sport & Tourism, vol. 29, no. 4, pp. 310-332, 2025, doi: 10.1080/14775085.2025.2595959.

[18] L. Li, "Research on the integration and development of traditional minority sports and tourism in Ganzi Prefecture," Academic Journal of Humanities & Social Sciences, vol. 7, no. 2, pp. 267-272, 2024, doi: 10.25236/AJHSS.2024.070238.

[19] X. Tan, Z. Liu, L. Shi, and X. Huang, "Geospatial analysis of sports tourism resources in China's urban clusters: a case study of the Sichuan-Chongqing region utilizing GIS and the geographic detector," Frontiers in Sports and Active Living, vol. 6, Art. no. 1496469, 2024, doi: 10.3389/fspor.2024.1496469.

[20] B. Mo, X. Zhang, W. Chen, R. Zhou, and J. Zhang, "Research on the spatial distribution characteristics and influencing factors of sports intangible cultural heritage in the Guangdong-Hong Kong-Macao Greater Bay Area," Scientific Reports, vol. 15, no. 1, Art. no. 27147, 2025, doi: 10.1038/s41598-025-10734-3.

[21] W. Kou and J. Zhai, "Spatial distribution patterns and influencing factors of sports intangible cultural heritage in China," Frontiers in Earth Science, vol. 13, Art. no. 1556652, 2025, doi: 10.3389/feart.2025.1556652.

[22] K. Zhang, X. Mei, and Z. Xiao, "Spatio-temporal evolution of sports tourism industry integration: A empirical analysis of Xinjiang in China," Plos one, vol. 19, no. 4, Art. no. e0300959, 2024, doi: 10.1371/journal.pone.0300959.

[23] S. Yu, K. Li, and G. Zhao, "An Improved Gated Graph Neural Network for Sports Tourism Recommendation: User Embedded Representations and Attention Mechanisms," Informatica, pp. 49(27), 2025, doi: 10.31449/inf.v49i27.8490.

[24] Q. Hu, P. Yang, J. Ma, M. Wang, and X. He, "The spatial differentiation characteristics and influencing mechanisms of intangible cultural heritage in China," Heliyon, pp. 10(22), 2024, doi: 10.1016/j.heliyon.2024.e38689.

[25] X. Li, "Determination of the temporal–spatial distribution patterns of ancient heritage sites in China and their influencing factors via GIS," Heritage Science, vol. 12, no. 1, pp. 1-14, 2024, doi: 10.1186/s40494-024-01258-6.

[26] C. Tang, L. Shangguan, L. Liu, and J Mei The model and path for digital cultural tourism to promote rural revitalization, "Journal of Resources and Ecology," 2024; 15(3): 528-540, doi: 10.5814/j.issn.1674-764x.2024.03.002.

[27] F.H.Research on Dynamic Mechanism and Management Mode of Sports Tourism Development in China, "Revista de Psicología del Deporte (Journal of Sport Psychology)," 2024; 33(2): 158-167, doi: 10.5814/rpd.33.2.158.